Polímeros
ISSN 1678-5169 (Online)
CC BY
https://doi.org/10.1590/0104-1428.20230126

Chemical and mechanical resistance of waterborne polyurethane/graphene (WPU/GO) nanocomposite coatings

Pietro Paolo de Oliveira e Silva[1]*, Enderson José Dias de Melo[1], Arthur Israel Carneiro Espíndola[2], Marcus Vinicius Fernandes Florentino[3], Ana Paula Lima da Silva[2], Elinaldo Neves dos Santos[3]

[1]Departamento de Física, Instituto Federal de Pernambuco – IFPE, Recife, PE, Brasil
[2]Departamento de Engenharia Civil, Instituto Federal de Pernambuco – IFPE, Recife, PE, Brasil
[3]Departamento de Engenharia Mecânica, Instituto Federal de Pernambuco – IFPE, Recife, PE, Brasil
**pietropaolo@recife.ifpe.edu.br*

Abstract

Waterborne polyurethane (WPU) coatings used for moisture protection of surfaces have been used broadly. They have been considered environmentally friendly because their synthesis releases less or no volatile organic compounds (VOCs) to the atmosphere. With the Covid-19 pandemic concerns, cleaning protocols of these surfaces have been applied and scientific knowledge about the effects of these liquids on WPU surfaces is necessary. In this work, diffusion experiments were performed using four liquids, in pure WPU and WPU filled with graphene oxide (GO). Detergent had the most severe effect on polyurethane films, causing severe cracks and weight loss. Diffusion parameters of HCl 5% and HCl 10% were greater in WPU/GO nanocomposites than in pure WPU. Mechanical tests under chemical aging showed that alcohol reduced most the tensile strength and Young modulus. Overall, GO protected the films for all liquid exposures, increasing their tensile strength and Young modulus.

Keywords: *covid-19 cleaners, diffusion parameters, graphene oxide, waterborne polyurethane, nanocomposites.*

How to cite: Silva, P. P. O., Melo, E. J. D., Espíndola, A. I. C., Florentino, M. V. F., Silva, A. P. L., & Santos, E. N. (2024). Chemical and mechanical resistance of waterborne polyurethane/graphene (WPU/GO) nanocomposite coatings. *Polímeros: Ciência e Tecnologia*, *34*(2), e20240016. https://doi.org/10.1590/0104-1428.20230126

1. Introduction

Polyurethanes (PUs) are a particularly important class of thermoset coatings, with widespread applications in the automotive, aerospace, industrial maintenance, wood, and plastic coatings fields. However, the coatings industry has become increasingly concerned with environmental issues, adopting attitudes to increasingly reduce the emission of volatile organic compounds (VOCs) into the atmosphere. One of these approaches is the replacement of solvent-based PU with water-based/waterborne PU (WPU)[1,2]. Waterborne coatings appear as an excellent option when concerns for the environment is a priority, as well as compliance with the environmental standards of each country[3,4]. Waterborne polyurethane dispersions have emerged as an important alternative to solvent-borne adhesives and coatings due to environmental concerns[5,6].

WPU coatings have properties desired by the industry, such as chemical resistance, flexibility and relative thermal and mechanical resistance. However, in some applications that demand higher levels at the limits of these properties, thermoset WPU films may not meet the demand[7]. The incorporation of nanofillers into the WPU matrix can eliminate this type of limitation, as the filler plays an important role in increasing the physicochemical properties of polymers and, therefore, can be used for the development of a new generation of composite materials. Clay, nano silica, cellulose nanocrystal, carbon nanotubes, graphene oxide (GO), reduced graphene oxide and graphene can be used for this purpose[8]. Among the various nanofillers employed in the fabrication of polymer nanocomposites, graphene and graphene-based materials such as GO have attracted significant attention to researchers and scientists due to their unique combination of properties[9-12]. Polymer nanocomposites based on PU and graphene-based materials have a great application opportunity in automobile body parts, flexible pipes, biomedical devices, paints, coating of wires and cables, protective coatings in the construction industry, etc[8].

Graphene oxide is capable of providing surprising improvements in material properties when used in a composite, even at a very low percentage (up to 1%w/w), acting as a multifunctional crosslinker as well as a filler. Researchers and scientists working around the world are curious to discover the hidden potential of this 2D nanomaterial in enhancing polyurethane properties[13,14]. Pokharel and Lee[15] demonstrated an improvement of 40.5% in tensile strength and 19% in elasticity of PU with the addition of 1%w/w of GO. The advantage of GO over graphene when incorporating into water-based PU is that, compared with graphene, GO is easy to be homogeneously dispersed in aqueous solution, which is attributed to the existence of a large number of oxygen-containing functional groups, such as hydroxyl, carboxyl, carbonyl and epoxy[16]. Nanomaterials such as nano-silica, nano-zinc oxide, nano-titanium dioxide, clay, and cellulose nanocrystals have been widely used to improve the properties of waterborne polyurethane[17].

Moreover, after the Covid-19 pandemic, frequent surface cleaning became mandatory mainly in public locations. In many cases, these surfaces are protected with WPU coating, as in civil constructions, since this polymer coating is used as a surface waterproof protection. Common cleaner liquids for this purpose include alcohols, diluted dishwashing detergents, HCl diluted in water (muriatic acid) and so on[18,19]. As a result, understanding the effects of these liquids exposure in polymeric coating properties plays an important role in polymer science.

In this regard, this work aims to study the effect of the exposure of four liquids (HCl 5%, HCl 10%, 70% Ethyl alcohol and 50% diluted detergent) in WPU and how the addiction of GO in WPU matrix can influence in this behavior, based in diffusion approach, tensile properties and infrared spectroscopy. No scientific work has been found in the database exploring this subject so far.

2. Materials and Methods

2.1 Materials

Waterborne polyurethane, a commercial grade provided from Holf Hacker®, was used as supplied. This product is used as a waterproof agent in civil buildings, applied as a coating in concrete surfaces, wood and floors.

2.2 GO Synthesis and WPU/GO preparation

GO Synthesis follows a modified Hummers method[20]. Natural graphite flakes (5.0 g - 140 mesh) was intercalated with 100 mL of a freshly prepared mixture of sulfuric-nitric acid (4:1 v/v) to yield graphite intercalation. The resulting mixture was stirred for 16 h, and then filtered through a Hirsch funnel. The resulting product was rinsed with deionized water (DI) until the filtrate reached neutrality and then dried in an oven for 24 h at 80 °C. The dried intercalated graphite was expanded by irradiation in a microwave oven (1.2 kW, Consul, Brazil) for 3-5 min. The expanded graphite was mixed with a 35% hydroalcoholic ethanol solution, followed by sonication for 5 min (50% amplitude) with an immersion ultrasonic probe (Sonics Vibra Cell Vc 505, 500W, 20 kHz, Sonics & Materials) at room temperature. The exfoliated graphite was filtered, washed with DI, air-dried for 24 h, and then dried at 80 °C overnight. An additional oxidation reaction was carried out using 1.0 g of exfoliated graphite with a solution of 0.5 g of $NaNO_3$ in 25 mL of concentrated H_2SO_4. The mixture was stirred for 40 min in an ice bath. $KMnO_4$ (3.0 g) was added, and additional stirring was carried on for an additional 2 h. The mixture was then left to rest at room temperature for 30 min, and excess H_2O_2 (5%) was added. The resulting mixture was rapidly heated up to 90 °C in a water bath and filtered through a Teflon™ membrane (Milipore VVLP type 0.1 μM). The residue was washed with DI, air-dried for 24 h, and then dried at 80 °C in an oven, yielding 3.15 g of GO.

WPU/GO thin films were prepared by directly mixing GO in the WPU solution as provided. Initially, the water content in the polyurethane solution was measured and subtracted in the calculation of GO ratio, as this water evaporates during the coalescence and cure of the WPU film when it dries. The WPU and WPU/GO solutions were cast in PTFE (polytetrafluoroethylene) molds and dried at room temperature (~28°C). The GO in specific ratio was added in a Becker containing WPU and put in vigorous magnetic stirrer for 2h. The GO ratios used in this work were 0.25, 0.5, and 1%w/w[7-12].

2.3 Diffusion parameter

Swelling experiments were performed at WPU or WPU/GO film samples immersed in four liquids, HCl 5%, HCl 10%, 70% ethyl alcohol and 50% diluted solution of a commercial dishwashing detergent in deionized (DI) water. The films used in this test measured approximately 0.8x10x20 mm and were used in triplicate for each liquid. Film samples were placed in glass flasks with about 100 mL of each liquid at room temperature for an extended period (up to 1500 hours), until the plateau region reached stability and could be clearly identified. At regular intervals, the samples were removed from the liquid, carefully dried with paper towels, quickly weighed (APX-200 balance, 0.01mg precision, Denver Instruments), and then returned to the soaking bath. Sorption graphics of the samples can provide the diffusion parameters for surface-active liquids in the PU, using equations such as Fick's 2nd law of diffusion[21]:

$$\delta C_d \,/\, \delta t = D\left(\delta^2 C_d \,/\, \delta x^2\right) \tag{1}$$

where 'C_D' is the concentration of the diffusing substance, 'D' is the diffusion parameter and 't' is time. A solution to the above equation for diffusion in a flat sheet with surfaces maintained at a constant concentration is given by Crank's Equation[22] as:

$$M \;/\, M_\infty = 1 - \sum_{=0}^{\infty} 8/\pi^2\left(2n+1\right)^2 \times \exp(-D\left(2n+1\right)^2 \pi^2 t / L^2) \tag{2}$$

where 'L' is the thickness of the sheet, 'M_T' and 'M_∞' are, respectively, the mass of the diffusing substance after a given soaking time 't' and at the final sorption time (equilibrium) '∞'. The ratio M_t/M_∞ ratio in Equation 3 can be expressed as[21]:

$$M_t \,/\, M_\infty = \left(W_s - W_d\right) / \left(W_\infty - W_d\right) \tag{3}$$

where 'W_D' is the weight of the dry sample, 'W_S' is the sample weight after a given soaking time 't', and 'W_∞' is the sample weight in the sorption equilibrium. In short soaking times, the mass of the diffusing substance can be considered as proportional to √t. This approximation is called The Square-Root-of-Time law[23] or Stefan's approximation[21] which is given by Equation 4:

$$M_t \,/\, M_\infty = 4[Dt \,/\, \pi L^2]^{1/2} \tag{4}$$

A plot of $Mt/M\infty$ versus the square root of sorption time ($\sqrt{t}$) is generally termed as 'sorption curve' and '*D*' is calculated from the slope of the initial linear portion of this curve[21,24]. A Fickian-type diffusion is characterized by diffusion rates lower than polymer segmental relaxations, owing to various modes of interaction within the penetrant-polymer system, such as mechanical and structural interactions[21].

2.4 Tensile strength test

Stress-strain curves were obtained on an Intermetric IM100 mechanical test machine, using a crosshead speed of 20mm/min (ASTM D 882-18). The tests were conducted on pure WPU thin films and WPU/GO thin films in all GO ratio described above. The chosen film (optimal GO ratio) was the one that exhibited the best performance in the tensile tests. Tensile tests on aged WPU and WPU/GO films were performed under the same conditions, except that films were left immersed for 72h in the specific liquid prior the tensile tests for accelerated aging[25,26] The samples dimensions were approximately 0.8x10x100mm, obtained through casting in PTFE molds (the same method described on section 2.2 above).

2.5 FTIR

Infrared spectra were acquired using the FTIR Jasco Spectrophotometer, model 4600, with 32 scans, a resolution of 4 cm^{-1}, in transmission mode within the range of 4000-400 cm^{-1}, employing the Attenuated Total Reflectance (ATR) technique. Aged films were tested as well under the same conditions as the mechanical tests.

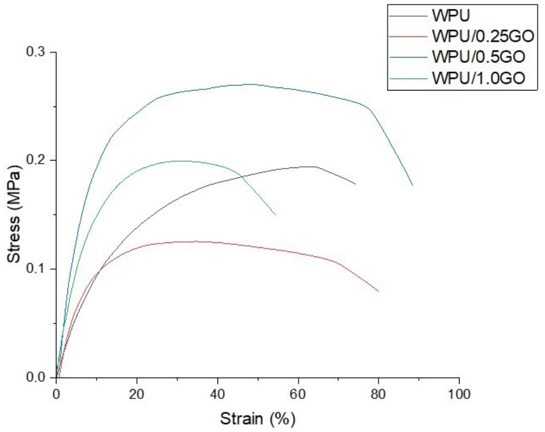

Figure 1. Stress-strain curves for pure waterborne polyurethane and WPU/GO nanocomposites.

3. Results and Discussions

3.1 Tensile strength tests for best GO ratio in the WPU matrix

Tensile strength tests were initially performed on WPU matrices with varying GO ratios to determine the ratio that yielded the best mechanical performance. Figure 1 shows the stress-strain curves for pure WPU and WPU/GO formulations. As evident from the curves, the optimal GO ratio in the WPU matrix, considering mechanical performance, was 0.5%w/w. The maximum tensile strength for this ratio was approximately 0.28 MPa, whereas for the pure WPU and other GO ratios, it remained below 0.20 MPa. This represents a 40% improvement in this property. The maximum strain (elongation at break) for the 0.5% ratio also achieved the best value, reaching 77%, indicating a 25% improvement compared to pure WPU. Zhang et al.[14] has found a significant improvement in the mechanical strength of WPU using a functionalized GO at 0.5 wt% as the optimal ratio. Wan and Chen[27] demonstrated an overall improvement in the mechanical resistance of WPU/GO with increasing GO content. Considering that 0.5% w/w of GO content in WPU exhibited the best overall mechanical behavior, this ratio was selected for subsequent tests in this study and will be referred to as WPU/0.5GO henceforth. Figure 2 and Table 1 depict mechanical properties of the films based on GO ratio.

3.2 Diffusion parameters

The D values are crucial for predicting the material's susceptibility to environmental stress cracking (ESC),

Table 1. Mechanical properties of WPU and WPU/GO films.

	Tensile Strength (MPa)	Young Modulus (MPa)	Elongation at Break (%)
WPU	0.22±0.04	1.79±0.26	62.85±13.74
WPU/0.25GO	0.125±0.02	1.87±0.11	70.2±5.32
WPU/0.5GO	0.28±0.02	2.98±0.27	77.36±8.01
WPU/1.0GO	0.2±0.03	2.21±0.18	54.15±2.71

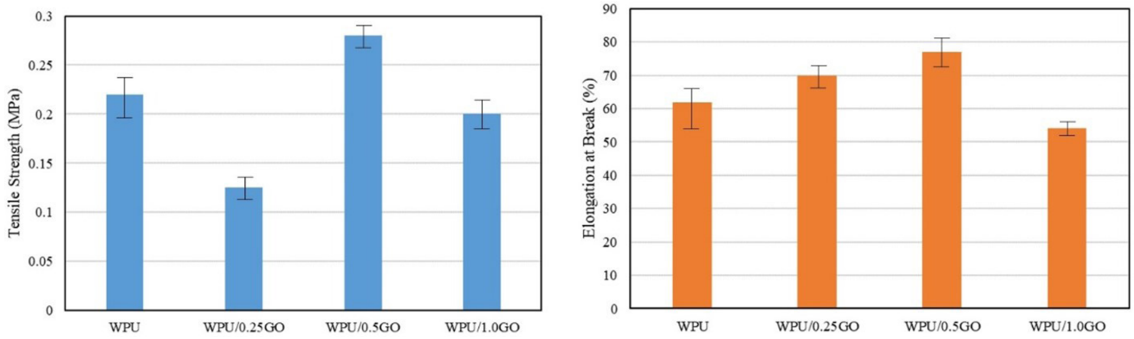

Figure 2. Tensile Strength and strain capacity of WPU and WPU/GO nanocomposites.

which can ultimately lead to polymer rupture and failure under operational conditions[28]. To measure this parameter, sorption tests were conducted, and the obtained sorption curves are depicted in the figures below. For WPU and WPU/0.5GO immersed in HCl 5%, the diffusion parameter found were $1.03 \times 10^{-8} \pm 20\%$ m^2/s and $8.63 \times 10^{-8} \pm 24\%$ m^2/s, respectively. It is noteworthy that, at the beginning of the sorption process, WPU chains underwent a chemical reaction with HCl, contributing to the formation of bubbles on the surface of WPU films and resulting in weight loss rather than weight gain. This effect was observed in both pure WPU and WPU/0.5GO films, as shown in Figure 3 (left). The phenomenon of bubble formation has been noted by other researchers and attributed to a chemical reaction between the acid and polyurethane material[29]. Waterborne polyurethanes contain various functional groups, such as hydroxyl and carbonyl groups, which can react with acids like hydrochloric acid. The acid can initiate a reaction with these functional groups, leading to the formation of gas bubbles as a byproduct[29]. Additionally, the composition and structure of the waterborne polyurethane can influence the formation of bubbles when exposed to hydrochloric acid. For example, glucose and sulfamate double-modified biodegradable waterborne polyurethane have been shown to have better acid resistance properties, which may affect the formation of bubbles[30]. Similarly, cationic waterborne polyurethanes synthesized from waste frying oil have been found to exhibit resistance to both acid and alkaline environments, which may impact bubble formation[31]. Despite this, after the weight loss, it can be observed that Fickian diffusion behavior takes place, typically indicating liquid uptake and a plateau region after saturation[28,32]. Although graphene oxide promoted better mechanical behavior, for HCl 5%, WPU thin films became more susceptible to swelling and liquid diffusion. There are no references regarding measuring diffusion parameters in WPU or in WPU/GO nanocomposites. However, this behavior can be attributed to the oxygenated groups in GO structure that can react with oxygen in aqueous media, subtracting the reinforcement structure of GO in WPU matrix[33]. The same trend can be observed for diffusion parameters of HCl 10% in WPU and WPU/0.5GO films. Figure 3 (right) depicts sorption curves for WPU and WPU/0.5GO immersed in HCl 10%. The diffusion parameters for HCl 10% in WPU and WPU/0.5GO were respectively $9.96 \times 10^{-8} \pm 20\%$ and $5.91 \times 10^{-7} \pm 14\%$ m^2/s. Figure 4 shows bubbles formed in WPU surfaces when immersed in HCl medium.

For WPU and WPU/0.5GO immersed in diluted detergent, a severe degradation process took place. Nevertheless, it was observed that graphene oxide protected the films to a certain extent, because in the pure waterborne polyurethane thin films, after 76 hours of immersion, the films started do

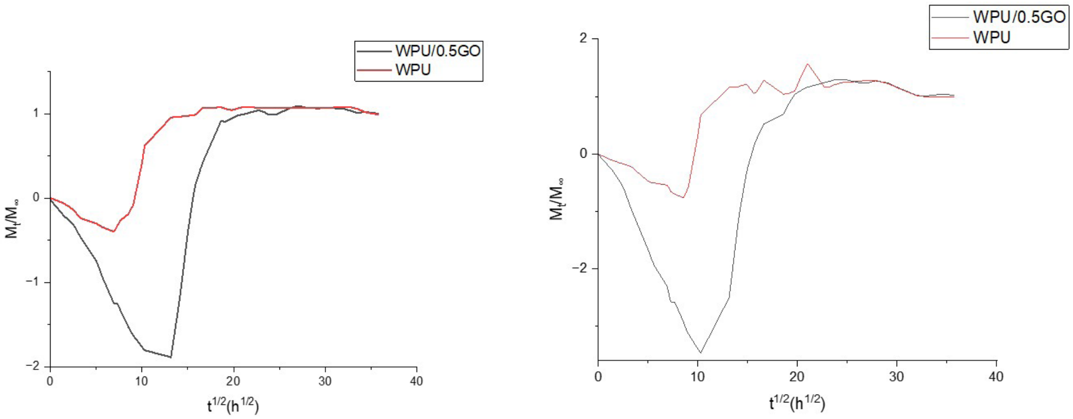

Figure 3. Sorption curve for WPU and WPU/0.5GO immersed in HCl 5% (left) and HCl 10% (right).

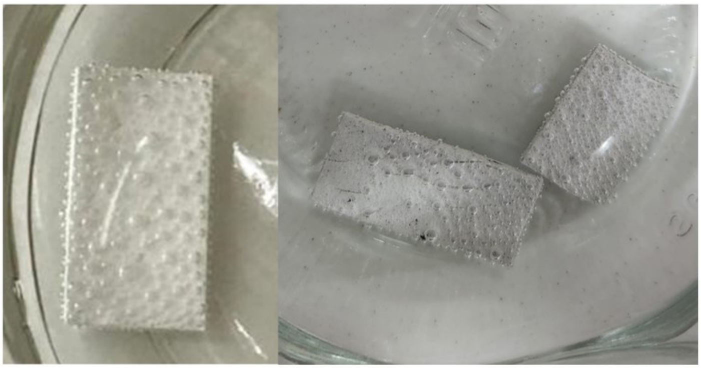

Figure 4. WPU and WPU/0.5GO films exhibiting bubble formation when immersed in diluted HCl due chemical reactions.

degrade, losing weight over time and visually cracking and breaking into small pieces. In the films containing GO, this process took place as well but only started after 226 hours of liquid exposure, and the mass loss was less pronounced (i.e. the slope of the curve was smaller). This behavior classifies the swelling phenomenon as non-Fickian[28]. Figure 5 shows the variation in the films' weight over time, and Figure 6 presents sample pictures depicting the degradation process occurring in the films.

Finally, for 70% ethyl alcohol, the D values for WPU and WPU/0.5GO were respectively $9.05\text{x}10^{-9}$ ±17.7% and $5.71\text{x}10^{-9}$ ±20.1% m^2/s. Here, as in detergent, GO improved the resistance of the polyurethane chain to alcohol uptake by about 37%. However, contrary to the behavior in detergent, WPU and WPU/GO films underwent minor degradation after reaching the inflection point of the swelling curve. However, contrary to the behavior in detergent, WPU and WPU/GO films underwent minor degradation after reaching the inflection point of the swelling curve. It is important to highlight that for COVID-19 disease, 70% ethyl alcohol is the most commonly used liquid for surface sterilization[34,35]. Figure 7 shows sorption curves for 70% alcohol in WPU and WPU/0.5GO.

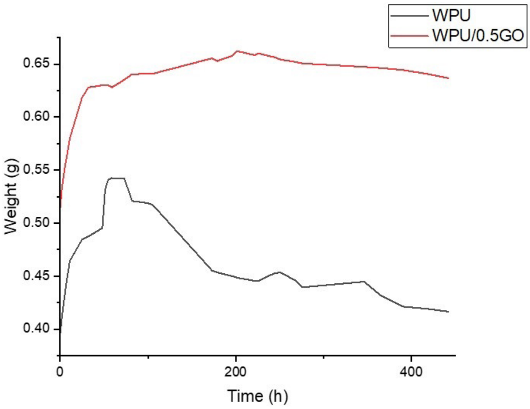

Figure 5. Weight variation of WPU and WPU/0.5GO immersed in diluted detergent.

3.3 Mechanical tests after accelerated aging

Mechanical tests were performed on pure WPU and WPU/0.5GO under 72h of aging in each of the four liquids. Figure 8 displays stress-strain curves for all cases. Overall, GO has improved mechanical tensile strength, Young's modulus and elongation at break. These results are consonant with other research studies[27,36,37] and demonstrate the significant impact of GO on improving the mechanical properties of polymeric matrices. WPU/0.5GO outperformed pure WPU in terms of mechanical performance under chemical aging. Furthermore, among all the liquids, 70% alcohol had a more pronounced effect on decreasing the tensile strength of WPU thin films, even though detergent was the most degrading liquid in swelling experiments. Although this behavior may appear surprising, similar behavior have been observed in other polymeric systems. This likely occurred because the polar part of PU chain, as C=O, was attacked by the high polarity part of alcohol chain. This phenomenon was attributed to a match between dispersion and polar cohesion energy of Hansen's solubility parameters of ethyl alcohol and polyurethane[28,38]. For PU, the energy from polar intermolecular forces δ_P is 9,3 and for ethyl alcohol is 8.8 MPa$^{0.5}$ and from dispersive δ_D is 18.1 and 15.8 MPa$^{0.5}$ [39]. WPU, under 70% alcohol aging, became significantly more deformable, as its strain capacity increased by almost 100% compared to pure WPU without chemical aging. It is worth noting that despite HCl 5% and 10% having a diffusion parameter greater in WPU/GO than in pure WPU, for mechanical tests, GO improved WPU mechanical resistance. Tensile strength for pure WPU decreased more when immersed in HCl than WPU/GO immersed in the same solution.

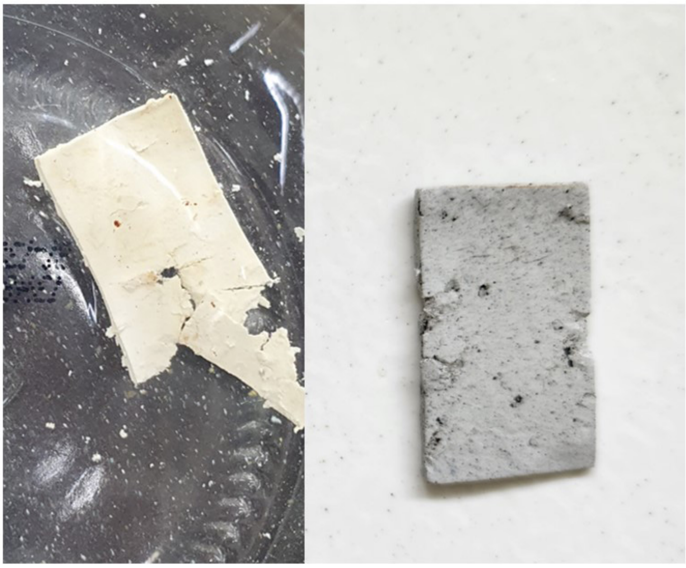

Figure 6. WPU and WPU/GO films cracked after detergent immersion.

Table 2 summarizes mechanical properties from tensile stress experiments.

3.4 FTIR analysis

Figure 9 displays FTIR spectra of graphite, GO, WPU and WPU/0.5GO. The GO spectrum exhibits oxygenated functional groups aggregated in the graphite matrix after all the oxidation steps used to transform pure graphite powder into graphene oxide. Absorption peaks for GO have been identified at 1086 cm^{-1} (C–O stretching), 1721 cm^{-1} (C=O stretching) and 3296 cm^{-1} (O-H stretching)[40]. The spectra of WPU and WPU/0.5GO are similar, as the amount of GO in the WPU matrix is very small, and the GO peaks overlap with the more intense bands of WPU. A weak peak was observed at approximately 3350 cm^{-1}, corresponding to the N–H stretching vibration. The two duplets observed at 2872 and 2954 cm^{-1} are assigned to the C–H stretching vibrations of urethane bonds. The peak at 1725 cm^{-1} corresponds to C=O stretching from the urethane group. The N–H (Symmetrical bending) band from urea group at 1465 cm^{-1} was observed. The peak at 1160 cm^{-1} is attributed to C–O–C (ether) asymmetrical stretching[41,42].

Figure 10 illustrates the FTIR spectra for WPU and WPU/0.5GO in various scenarios, without chemical aging and with chemical aging. It is evident that the spectra bear a striking resemblance to each other. This similarity suggests that chemical reactions did not occur when the films were immersed in the liquids, with the exception of the peak at 876 cm^{-1}, attributed to bending vibration from C-O-C. Notably, this peak disappears in films aged in HCl[43]. This can be explained by the fact that bubble formation in the film surfaces were formed, as discussed in section 3.2 above, and chemical reactions with the HCl and WPU took place. The chemical reaction of hydrochloric acid with the C-O-C group from polyurethane involves the cleavage of the C-O-C bond that can result in the degradation of the polyurethane structure and the formation of by-products. This finding aligns with the outcomes discussed in the mechanical properties section. Additionally, in HCl and detergent media, the spectra present a more intense and wider peak in the region 3200-3600 cm^{-1}. This appears to indicate additional formation of -OH broader peaks in the region, and suggests chemical reactions between the media and WPU

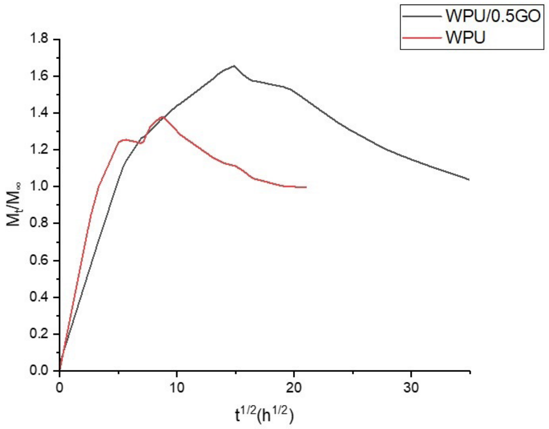

Figure 7. Sorption curve for WPU and WPU/0.5GO immersed in 70% ethyl alcohol.

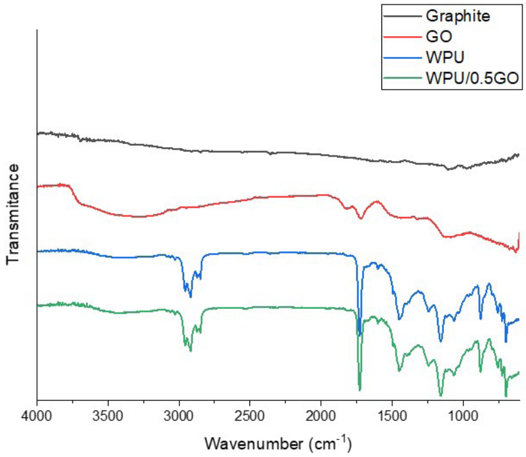

Figure 9. FTIR spectra of graphite, GO, WPU and WPU/0.5GO.

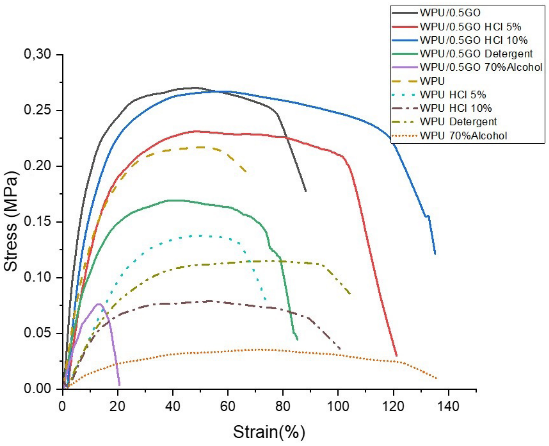

Figure 8. Stress-strain curves for WPU and WPU/0.5GO in all scenarios.

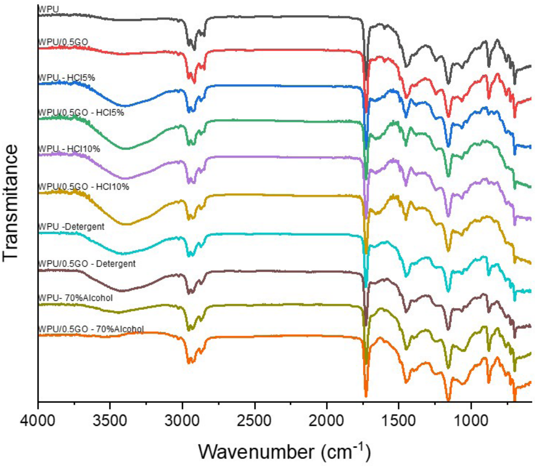

Figure 10. FTIR spectra for WPU and WPU/0.5GO in all scenarios.

Table 2. Mechanical properties of WPU and WPU/0.5GO in all scenarios.

	Tensile Strength (MPa)	Young Modulus (MPa)	Elongation at Break (%)
WPU	0.22±0.04	1.79±0.26	62.85±13.74
WPU HCl 5%	0.14±0.01	0.52±0.12	58.09±6.48
WPU HCl 10%	0.10±0.02	0.43±0.19	94.52±3.63
WPU Detergent	0.08±0.02	0.42±0.18	106.53±10.63
WPU 70% Alcohol	0.04±0.01	0.21±0.11	116.68±10.64
WPU/0.5GO	0.28±0.02	2.98±0.27	77.36±8.01
WPU/0.5GO HCl 5%	0.24±0.02	1.72±0.22	110.00±16.07
WPU/0.5GO HCl 10%	0.26±0.01	2.61±0.34	135.79±17.05
WPU/0.5GO Detergent	0.17±0.01	1.48±0.31	66.72±9.56
WPU/0.5GO 70% Alcohol	0.07±0.02	1.11±0.21	15.37±1.70

matrix. For HCl, these reactions can lead to the formation of hydroxyl groups (OH) and typically involve the breaking of existing bonds in polyurethane, especially those containing oxygen atoms, such as esters and urethane groups. The H^+ ions from hydrochloric acid can react with the functional groups in polyurethane, leading to the release of water and the formation of new bonds. Consequently, hydroxyl groups may be incorporated into the structure, depending on the specific characteristics of the polyurethane and the reaction conditions. These modifications in the chemical structure can have significant effects on the physical and mechanical properties of polyurethane[44,45].

4. Conclusions

Previous mechanical tensile tests indicated that a GO concentration of 0.5%w/w was optimal in the WPU matrix. Sorption tests revealed that common Covid-19 cleaners used in this study should be avoided for prolonged exposure on surfaces protected with waterborne polyurethane (WPU) coatings, as WPU tends to absorb them. Among the four liquids, diluted dishwasher detergent proved to be the most aggressive during extended exposure, leading to severe cracks in WPU films. Surprisingly, graphene oxide provided overall protection from degradation, even exhibiting greater diffusion parameters than pure WPU for HCl solutions. In mechanical tensile experiments under chemical aging, WPU/GO nanocomposites demonstrated greater tensile strength and Young modulus, even when exposed to liquids. Despite 50% diluted detergent being the most aggressive liquid for extended WPU exposure, 70% ethyl alcohol emerged as the most aggressive solution, reducing the mechanical performance of both WPU and WPU/GO nanocomposite. This phenomenon was attributed to Hansen solubility parameters. FTIR spectra suggests that HCl promotes a chemical reaction in WPU main chain, leading to bubble formation and the suppression of C-O-C bands. Therefore, liquids such HCl 5%, HCl 10%, detergent solution and 70% alcohol- typical substances used for cleaning surfaces against biological contamination likeSARS-CoV-2- should be avoided in contact with WPU coatings. Notably, GO demonstrated the ability to enhance the overall resistance of WPU to these liquids.

5. Author's Contribution

- **Conceptualization** – Pietro Paolo de Oliveira e Silva.
- **Data curation** – Pietro Paolo de Oliveira e Silva; Enderson José Dias de Melo; Elinaldo Neves dos Santos.
- **Formal analysis** – Pietro Paolo de Oliveira e Silva; Arthur Israel Carneiro Espíndola; Marcus Vinicius Fernandes Florentino.
- **Funding acquisition** – Pietro Paolo de Oliveira e Silva.
- **Investigation** – Pietro Paolo de Oliveira e Silva; Enderson José Dias de Melo; Arthur Israel Carneiro Espíndola; Elinaldo Neves dos Santos.
- **Methodology** – Pietro Paolo de Oliveira e Silva; Enderson José Dias de Melo; Marcus Vinicius Fernandes Florentino; Ana Paula Lima da Silva.
- **Project administration** – Pietro Paolo de Oliveira e Silva.
- **Resources** – Pietro Paolo de Oliveira e Silva.
- **Software** – NA.
- **Supervision** – Pietro Paolo de Oliveira e Silva.
- **Validation** – Pietro Paolo de Oliveira e Silva; Arthur Israel Carneiro Espíndola.
- **Visualization** – Pietro Paolo de Oliveira e Silva; Enderson José Dias de Melo; Ana Paula Lima da Silva.
- **Writing – original draft** – Pietro Paolo de Oliveira e Silva.
- **Writing – review & editing** – Pietro Paolo de Oliveira e Silva.

6. Acknowledgements

The authors thank Wolf Hacker & cia Ltda for polyurethane supplying.

7. References

1. Zhou, X., Fang, C., Lei, W., Su, J., Li, L., & Li, Y. (2017). Thermal and crystalline properties of waterborne polyurethane by in situ water reaction process and the potential application as biomaterial. *Progress in Organic Coatings*, *104*, 1-10. http://doi.org/10.1016/j.porgcoat.2016.12.001.
2. Noreen, A., Zia, K. M., Zuber, M., Tabasum, S., & Saif, M. J. (2016). Recent trends in environmentally friendly water-borne polyurethane coatings: A review. *Korean Journal of Chemical Engineering*, *33*(2), 388-400. http://doi.org/10.1007/s11814-015-0241-5.
3. Liu, Z., Wu, B., Jiang, Y., Lei, J., Zhou, C., Zhang, J., & Wang, J. (2018). Solvent-free and self-catalysis synthesis and properties of waterborne polyurethane. *Polymer*, *143*, 129-136. http://doi.org/10.1016/j.polymer.2018.04.010.
4. Liu, X., Hong, W., & Chen, X. (2020). Continuous production of water-borne polyurethanes: a review. *Polymers*, *12*(12), 2875. http://doi.org/10.3390/polym12122875. PMid:33266183.
5. Alvarez, G. A., Fuensanta, M., Orozco, V. H., Giraldo, L. F., & Martín-Martínez, J. M. (2018). Hybrid waterborne polyurethane/acrylate dispersion synthesized with bisphenol

a-glicidylmethacrylate (bis-gma) grafting agent. *Progress in Organic Coatings*, *118*, 30-39. http://doi.org/10.1016/j.porgcoat.2018.01.016.

6. Luo, S., Yang, K., Zhong, Z., Wu, X., & Ren, T. (2018). Facile preparation of degradable multi-arm-star-branched waterborne polyurethane with bio-based tannic acid. *RSC Advances*, *8*(66), 37765-37773. http://doi.org/10.1039/C8RA07875K. PMid:35558615.
7. Cai, D., Yusoh, K., & Song, M. (2009). The mechanical properties and morphology of a graphite oxide nanoplatelet/polyurethane composite. *Nanotechnology*, *20*(8), 085712. http://doi.org/10.1088/0957-4484/20/8/085712. PMid:19417473.
8. Bera, M., & Maji, P. K. (2017). Effect of structural disparity of graphene-based materials on thermo-mechanical and surface properties of thermoplastic polyurethane nanocomposites. *Polymer*, *119*, 118-133. http://doi.org/10.1016/j.polymer.2017.05.019.
9. Song, W., Wang, B., Fan, L., Ge, F., & Wang, C. (2019). Graphene oxide/waterborne polyurethane composites for fine pattern fabrication and ultrastrong ultraviolet protection cotton fabric via screen printing. *Applied Surface Science*, *463*, 56-65.
10. Kumar, A., Sharma, K., & Dixit, A. R. (2019). A review of the mechanical and thermal properties of graphene and its hybrid polymer nanocomposites for structural applications. *Journal of Materials Science*, *54*(8), 5992-6026. http://doi.org/10.1007/s10853-018-03244-3.
11. Kumar, A., Sharma, K., & Dixit, A. R. (2022). Effects of various functional groups in graphene on the tensile and flexural properties of epoxy nanocomposites: a comparative study. *Fullerenes, Nanotubes, and Carbon Nanostructures*, *30*(11), 1123-1133. http://doi.org/10.1080/1536383X.2022.2077332.
12. Kumar, A., Sharma, K., & Dixit, A. R. (2023). Tensile, flexural and interlaminar shear strength of carbon fiber reinforced epoxy composites modified by graphene. *Polymer Bulletin*, *80*(7), 7469-7490. http://doi.org/10.1007/s00289-022-04413-w.
13. Kale, M. B., Luo, Z., Zhang, X., Dhamodharan, D., Divakaran, N., Mubarak, S., Wu, L., & Xu, Y. (2019). Waterborne polyurethane/graphene oxide-silica nanocomposites with improved mechanical and thermal properties for leather coatings using screen printing. *Polymer*, *170*, 43-53. http://doi.org/10.1016/j.polymer.2019.02.055.
14. Zhang, F., Liu, W., Wang, S., Jiang, C., Xie, Y., Yang, M., & Shi, H. (2019). A novel and feasible approach for polymer amine modified graphene oxide to improve water resistance, thermal, and mechanical ability of waterborne polyurethane. *Applied Surface Science*, *491*, 301-312. http://doi.org/10.1016/j.apsusc.2019.06.148.
15. Pokharel, P., & Lee, D. S. (2014). High performance polyurethane nanocomposite films prepared from a masterbatch of graphene oxide in polyether polyol. *Chemical Engineering Journal*, *253*, 356-365. http://doi.org/10.1016/j.cej.2014.05.046.
16. Cao, J., & Wang, C. (2017). Multifunctional surface modification of silk fabric via graphene oxide repeatedly coating and chemical reduction method. *Applied Surface Science*, *405*, 380-388. http://doi.org/10.1016/j.apsusc.2017.02.017.
17. Kong, L., Xu, D., He, Z., Wang, F., Gui, S., Fan, J., Pan, X., Dai, X., Dong, X., Liu, B., & Li, Y. (2019). Nanocellulose-reinforced polyurethane for waterborne wood coating. *Molecules*, *24*(17), 3151. http://doi.org/10.3390/molecules24173151. PMid:31470628.
18. Jing, J. L. J., Yi, T. P., Bose, R. J. C., McCarthy, J. R., Tharmalingam, N., & Madheswaran, T. (2020). Hand sanitizers: a review on formulation aspects, adverse effects, and regulations. *International Journal of Environmental Research and Public Health*, *17*(9), 3326. http://doi.org/10.3390/ijerph17093326. PMid:32403261.
19. Sharafi, S. M., Ebrahimpour, K., & Nafez, A. (2021). Environmental disinfection against covid-19 in different areas of health care facilities: a review. *Reviews on Environmental Health*, *36*(2), 193-198. http://doi.org/10.1515/reveh-2020-0075. PMid:32845869.
20. Lima, T. B. S., Silva, V. O., Araujo, E. S., & Araujo, P. L. B. (2019). Polymer nanocomposites of surface-modified graphene. I: thermal and electrical properties of poly(vinyl alcohol)/aminoacidfunctionalized graphene. *Macromolecular Symposia*, *383*(1), 1800051. http://doi.org/10.1002/masy.201800051.
21. Ramani, R., Shariff, G., Thimmegowda, M. C., Sathyanarayana, P. M., Ashalatha, M. B., Balraj, A., & Ranganathaiah, C. (2003). Influence of gamma irradiation on the formation of methanol-induced micro-cracks in polycarbonate. *Journal of Materials Science*, *38*(7), 1431-1438. http://doi.org/10.1023/A:1022951926769.
22. Crank, J. S. (1975). *The mathematics of diffusion*. Oxford: Oxford University Press.
23. Tarcha, P. J. (Ed.). (1990). *Polymers for controlled drug delivery*. Boca Raton: CRC Press.
24. Al-Saidi, L. F., Mortensen, K., & Almdal, K. (2003). Environmental stress cracking resistance: behavior of polycarbonate in different chemicals by determination of the time-dependence of stress at constant strains. *Polymer Degradation & Stability*, *82*(3), 451-461. http://doi.org/10.1016/S0141-3910(03)00199-X.
25. Oasmaa, A., & Kuoppala, E. (2003). Fast pyrolysis of forestry residue. 3. Storage stability of liquid fuel. *Energy & Fuels*, *17*(4), 1075-1084. http://doi.org/10.1021/ef030011o.
26. Fuensanta, M., Khoshnood, A., Rodríguez-Llansola, F., & Martín-Martínez, J. M. (2020). New waterborne polyurethane-urea synthesized with ether-carbonate copolymer and amino-alcohol chain extenders with tailored pressure-sensitive adhesion properties. *Materials*, *13*(3), 627. http://doi.org/10.3390/ma13030627. PMid:32023838.
27. Wan, T., & Chen, D. (2018). Mechanical enhancement of self-healing waterborne polyurethane by graphene oxide. *Progress in Organic Coatings*, *121*, 73-79. http://doi.org/10.1016/j.porgcoat.2018.04.016.
28. Silva, P. P. O., Araújo, P. L. B., Silveira, L. B. B., & Araújo, E. S. (2017). Environmental stress cracking in gamma-irradiated polycarbonate: a diffusion approach. *Radiation Physics and Chemistry*, *130*, 123-132. http://doi.org/10.1016/j.radphyschem.2016.08.006.
29. Yan, J., Li, X., Zhang, X., Liu, S., Zhong, F., Zhang, J., Zhang, Q., & Yan, Y. (2022). Metallo-polyelectrolyte-based waterborne polyurethanes as robust HCl corrosion inhibitor mediated by inter/intramolecular hydrogen bond. *ACS Applied Polymer Materials*, *4*(5), 3844-3854. http://doi.org/10.1021/acsapm.2c00306.
30. Wu, G., Li, Y., Yang, Z., & Zhang, H. (2021). Preparation and characterization of glucose and sulfamate double-modified biodegradable waterborne polyurethane. *ChemistrySelect*, *6*(31), 8140-8149. http://doi.org/10.1002/slct.202101706.
31. Phunphoem, S., Saravari, O., & Supaphol, P. (2019). Synthesis of cationic waterborne polyurethanes from waste frying oil as antibacterial film coatings. *International Journal of Polymer Science*, *2019*, 2903158. http://doi.org/10.1155/2019/2903158.
32. Dolmaire, N., Espuche, E., Méchin, F., & Pascault, J.-P. (2004). Water transport properties of thermoplastic polyurethane films. *Journal of Polymer Science. Part B, Polymer Physics*, *42*(3), 473-492. http://doi.org/10.1002/polb.10716.
33. Buszek, R. J., Barker, J. R., & Francisco, J. S. (2012). Water effect on the OH + HCl reaction. *The Journal of Physical Chemistry A*, *116*(19), 4712-4719. http://doi.org/10.1021/jp3025107. PMid:22563978.
34. Berardi, A., Perinelli, D. R., Merchant, H. A., Bisharat, L., Basheti, I. A., Bonacucina, G., Cespi, M., & Palmieri, G. F. (2020). Hand sanitisers amid covid-19: A critical review

of alcohol-based products on the market and formulation approaches to respond to increasing demand. *International Journal of Pharmaceutics*, *584*, 119431. http://doi.org/10.1016/j.ijpharm.2020.119431. PMid:32461194.

35. Hashemi, F., Hoepner, L., Hamidinejad, F. S., Haluza, D., Afrashteh, S., Abbasi, A., Omeragić, E., Imamović, B., Rasheed, N. A., Taher, T. M. J., Kurniasari, F., Wazqar, D. Y., Apalı, Ö. C., Yildirim, A. D., Zhao, B., Kalikyan, Z., Guo, C., Valbuena, A. C., Mititelu, M., Pando, C. M., Saridi, M., Toska, A., Cuba, M. L., Kwadzokpui, P. K., Tadele, N., Nasibova, T., Harsch, S., Munkh-Erdene, L., Menawi, W., Evangelou, E., Dimova, A., Marinov, D., Dimitrova, T., Shalimova, A., Fouly, H., Suraya, A., Faquim, J. P. S., Oumayma, B., Annunziato, M. A., Lalo, R., Papastavrou, E., Ade, A. D., Caminada, S., Stojkov, S., Narvaez, C. G., Mudau, L. S., Rassas, I., Michel, D., Kaynar, N. S., Iqbal, S., Elshwekh, H., & Hossain, I. (2023). A comprehensive health effects assessment of the use of sanitizers and disinfectants during covid-19 pandemic: A global survey. *Environmental Science and Pollution Research International*, *30*(28), 72368-72388. http://doi.org/10.1007/s11356-023-27197-6. PMid:37166731.
36. Tounici, A., & Martín-Martínez, J. M. (2020). Addition of graphene oxide in different stages of the synthesis of waterborne polyurethane-urea adhesives and its influence on their structure, thermal, viscoelastic and adhesion properties. *Materials*, *13*(13), 2899. http://doi.org/10.3390/ma13132899. PMid:32605195.
37. Feng, J., Wang, X., Guo, P., Wang, Y., & Luo, X. (2018). Mechanical properties and wear resistance of sulfonated graphene/waterborne polyurethane composites prepared by in situ method. *Polymers*, *10*(1), 75. http://doi.org/10.3390/polym10010075. PMid:30966110.
38. Silva, P. P. O., Araujo, P. L. B., Lima, T. B. S., & Araujo, E. S. (2022). The influence of Environmental Stress Cracking (ESC) and gamma irradiation on the mechanical properties of polycarbonate: study of synergistic effects. *Materials Research*, *25*, e20210342. http://doi.org/10.1590/1980-5373-mr-2021-0342.
39. Hansen, C. M. (2007). *Hansen solubility parameters: a user's handbook*. Boca Raton: CRC Press. http://doi.org/10.1201/9781420006834.
40. Wang, Y., Shao, Y., Matson, D. W., Li, J., & Lin, Y. (2010). Nitrogen-doped graphene and its application in electrochemical biosensing. *ACS Nano*, *4*(4), 1790-1798. http://doi.org/10.1021/nn100315s. PMid:20373745.
41. Li, Y., Chen, S., Shen, J., Zhang, S., Liu, M., Lv, R., & Xu, W. (2021). Preparation and properties of biobased, cationic, waterborne polyurethanes dispersions from castor oil and poly (caprolactone) diol. *Applied Sciences*, *11*(11), 4784. http://doi.org/10.3390/app11114784.
42. Cai, G., Shi, M., Gao, J., & Yuan, L. (2019). Preparation and photochromic properties of waterborne polyurethane containing spirooxazine groups. *Journal of Applied Polymer Science*, *136*(7), 47067. http://doi.org/10.1002/app.47067.
43. Wang, Y., & Jin, L. (2018). Preparation and characterization of self-colored waterborne polyurethane and its application in eco-friendly manufacturing of microfiber synthetic leather base. *Polymers*, *10*(3), 289. http://doi.org/10.3390/polym10030289. PMid:30966324.
44. Song, J., Wu, G., Shi, J., Ding, Y., Chen, G., & Li, Q. (2010). Properties and morphology of interpenetrating polymer networks based on poly(urethane-imide) and epoxy resin. *Macromolecular Research*, *18*(10), 944-950. http://doi.org/10.1007/s13233-010-1009-8.
45. Gunashekar, S., & Abu-Zahra, N. (2015). Synthesis of functionalized polyurethane foam using bes chain extender for lead ion removal from aqueous solutions. *Journal of Cellular Plastics*, *51*(5-6), 453-470. http://doi.org/10.1177/0021955X14559255.

Received: Dec. 27, 2023
Revised: Mar. 08, 2024
Accepted: Mar. 26, 2024